# Sea transport of bananas in containers – Parameter identification for a temperature model

Reiner Jedermann [a], Martin Geyer [b], Ulrike Praeger [b], Walter Lang [a]

[a] Institute for Microsensors, -actors and –systems (IMSAS), University Bremen, Germany
[b] Leibniz-Institute for Agricultural Engineering Potsdam Bornim (ATB), Germany

**Please cite this article as:**
Jedermann, R., et al. Sea transport of bananas in containers – Parameter identification for a temperature model.
Journal of Food Engineering, Volume 115, Issue 3, April 2013, Pages 330–338,
http://dx.doi.org/10.1016/j.jfoodeng.2012.10.039

## Abstract:

Losses of product quality during the sea transport of bananas in containers are related to the emergence of hot spots. In order to analyze critical conditions, a spatial temperature profile was recorded ashore in a container loaded with banana pallets. The identification of a structured system model showed that it is possible to reduce the information on the measured temperature curves to a set of only two index values. These can be interpreted as factors for coupling to the air stream and for the amount of heat generated by biological processes per banana box. The width of gaps between pallets was identified as the major influence on the spatial temperature profile. Boxes from which the unwanted banana ripening heat cannot be channeled away by the cooling unit can be detected by the quotient of the index values.

**Keywords:** Temperature mapping; sea transport; hot spot; gap; reefer; green life; air flow

### Nomenclature

| | |
|---|---|
| $c_1$, $c_2$ | gain factors for output of corner model |
| fit | calculated curve fit between model and measured curve |
| $k_1$ | coupling factor for the corner of a box |
| $k_M$ | coupling factor for the center of a box |
| $k_P$ | gain factor for the generated heat |
| $norm()$ | Euclidean length of a vector containing a time series |
| $P_G(t)$ | generated respiration heat |
| $P_W(t)$ | exponential respiration heat term |
| $Q_{10}$ | change of heat production at a temperature change of 10 K |
| $T_1$, $T_2$ | time constants (corner) |
| $T_3$, $T_4$ | time constants (center of the box) |
| $u_1(t)$ | mixed input signal for corner model |
| $u_s(t)$ | temperature of the supply air |
| $x_1(t)$, $x_2(t)$ | outputs or states of the delay elements (corner model) |
| $x_3(t)$, $x_4(t)$ | outputs or states of the delay elements (center model) |
| $y^*$ | model output |
| $y'$ | measured value |
| $\overline{y'}$ | average over time |
| $y_E(t)$ | corner temperature |
| $y_M(t)$ | temperature of the center of the box |

# 1. Introduction

The transport of palletized bananas from Central America to Europe in reefer containers has been daily business for more than one decade now, but there is still a large number of containers holding products that arrive in a poor condition due to inadequate temperature management during transport (Billing et al., 1998; Tanner and Amos, 2003). A better understanding of temperature-related problems will have great advantages for the transport chain of bananas. Packing problems can be avoided. Containers in which a critical hot spot is detected can be scheduled for priority unloading upon arrival. Pallets which were cooled quickly during transport are expected to have a longer banana green life, meaning that they can be stored for a longer period of time until unwanted ripening starts. A warehouse management system, which is based on temperature history and not just simply on the arrival date, will further help to reduce losses.

During the ship passage of two weeks, the bananas are cooled down from approximately 25 °C to 14 °C. Initial tests with data loggers placed between the bananas at different positions in the container showed that there are large differences in the velocity of the cooling process (Figure 1):

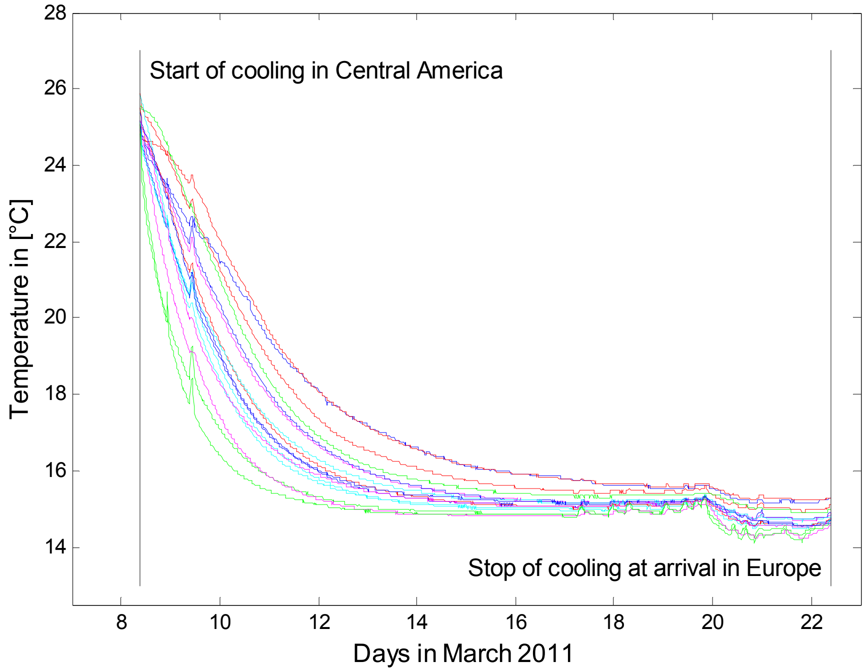


*Figure 1: Typical temperature curves for different positions in the container during sea transportation, measured between the bananas. The time required to cool down to 16 °C varies between 2 days and one week.*

A comparison of 5 temperature mappings in sea containers, carried out between 2008 and 2010 (Jedermann et al., 2010), showed that there is no unique position for the hot spot with the slowest decline in temperature. Other authors have come to the same result that it is quite difficult to predict the development and location of hot spots (Tanner and Amos, 2003; Moureh and Flick, 2004). Many studies are available about the modeling of air distribution in refrigeration rooms, in refrigerated trucks, vessels and containers (Rodriguez-Bermejo et al., 2007) using Computational Fluid Dynamics (CFD) and other tools.

In order to quantify the spatial dependency of the cooling performance, it is necessary to reduce the temperature over time function for each measurement position to an index value. Because a curve fitting with a simple exponential function led to high inaccuracies, we developed a model to describe the temperature behavior of palletized and boxed bananas.

We identified two major problems affecting the temperature distribution over time and over space in a packed banana container:

- Careless packing of the container at the farm results in uncontrolled gaps between the pallets inside the container, which leads to different air stream conditions between and in the cartons, to a change of air pressure and air volume of the cooling system, and thereby to a reduced cooling performance.
- Microbiological and mechanical defects in bananas can cause decay and ripening processes to start prematurely and thereby cause higher biological activity and heat production. The natural aging is slowed down by a controlled atmosphere and thereby the heat production is also reduced. A similar but smaller effect is achieved by a modified atmosphere if the banana batches are packed in special plastic film.

The structure of our model was selected in such a way that the two problems above are represented by two different model parameters.

In order to verify our modeling approach, we carried out a spatial temperature mapping with 138 data loggers. Because the installation of such a lavish setup was not feasible in Central America, we had to do the test ashore in Europe (section 2). After the test we developed a state-space model (section 3), identified the model parameters from the field test data, and analyzed the influence of gaps between the pallets and of other factors on the spatial temperature distribution (section 4).

# 2. Material and methods

For our tests we used pallets with bananas that were packed according to the following schema, which is common practice by the Dole company: batches of 18.4 kg bananas were each packed first in plastic film then in carton boxes at the farm in Central America. The plastic film prevents weight or moisture loss caused by the flow of the cooling air. The bags are normally completely closed to generate a modified atmosphere with increased carbon dioxide concentration. For transports under controlled atmosphere (CA) conditions, a generator on the ship supplies an atmosphere with $O_2$ decreased to 3% and $CO_2$ increased to 4.5%. In this case, the plastic film must have some small holes through which the CA can penetrate into a box.

The boxes were palletized for transport. Each pallet contained 880 kg of bananas in 48 boxes, placed in 6 stacks of 8 tiers height. During transport the bananas were cooled down to 14 °C.

After arrival in Europe, 16 pallets were taken out of the standard transport process. The pallets were unpacked and the plastic film inside the carton was opened in order to insert a sensor (Figure 2) and closed again. The bananas were already two weeks old at the start of the test, due to preliminary transport, but still green and in a good condition.

After stacking the boxes back on the pallets, the pallets were re-loaded to a 40-foot reefer container. The ambient temperature during the test in January 2012 was between 0.5°C and 6°C. The container was equipped with a new Thermoking Magnum Plus cooling unit (Ingersoll Rand, 2008) with an MP4000 controller, which allows the set point to be remotely adjusted. The unit has a nominal cooling capacity of 16.6 kW at 21.1 °C return air temperature. The evaporator fan has a maximum capacity of 5480 $m^3$ per hour at 50 Hz power supply. The test was carried out at the facilities of our project partner Dole in Stelle, close to Hamburg, Germany.

*Figure 2: Positioning the iButton temperature loggers between the bananas approximately at the center of the banana box. The plastic film was opened to install the temperature logger.*

In order to simulate the cooling process, we had to re-warm the bananas in our test container from the transport temperature of 14 °C to 16 °C over 32 hours by switching the set point. This temperature change slightly increases the respiration of the fruits, but did not produce any visible changes of the green ripe status. Afterwards, the bananas were cooled to 13 °C over 45 hours. Setting a wider temperature range was not possible because lower temperatures could damage the fruit by chilling injuries and higher temperatures could initiate an unwanted ripening process. During the last day of the experiment, the set point was switched again over 4 hours to 16 °C in order to test the short term reaction of the box corners. The measured temperature of the supply air reacted to step-wise changes of the set point with a delay time between 5 and 10 minutes.

The spatial temperature profile of the container was measured by 138 iButton temperature data loggers (Maxim Integrated Products, USA) with a measurement interval of 150 seconds. The iButtons can record up to 4000 temperature measurements. The accuracy of the iButtons was verified in a climatic chamber after the test. At 13 °C the iButtons showed an offset of +0.18 °C with a standard deviation of $\sigma$=0.07 °C. Only 4% of the iButtons had a deviation higher than $\pm 2 \cdot \sigma$. The measured offsets were subtracted from the measurement values. The reaction time of the iButton data loggers was estimated during an earlier experiment in a climatic chamber to approximately 2 minutes.

The iButton data loggers were placed either in the center between the bananas or in the free space in the corners of the boxes:

- Fifty-six data loggers were placed in the corners of the boxes in the fifth vertical tier counted from the bottom. These corner sensors react within a few hours or less to temperature changes in the cooling air. They can indicate after a short measurement time how well the box is connected to the air stream.
- Sixty-three data loggers were placed in the centers of the boxes in tier 5. Sensors in the center react only within days to temperature changes. But the temperature in the center has to be known to evaluate effects on the duration of the remaining green life of the bananas.

The remaining loggers were used to measure the temperature in different tiers as well as the supply and return air.

Additional wireless sensors provided temperature measurements in the container via remote online access. Because the wireless sensors reacted much more slowly to temperature changes due to their thermal mass, and because their SHT75 sensor element from Sensirion (Staefa ZH, Switzerland) had a higher measurement error, these data were not used for the thermal modeling of the container.

Figure 3 depicts the positions of the pallets inside the test container. Half of the pallets are turned through 90° in order to make best use of the available space. Normally 20 pallets are loaded per 40-foot container. For the trials in Stelle we had to reduce the number of pallets to 16 to provide space for additional measurement equipment. The free space between pallet stacks and the back door was closed by an isolated partition wall. Because the width of the container (2.29 m) is 4 cm larger than the sum of the width and length of two pallets, gaps between the pallets could not be avoided. In our test setup, we tried to create a hot spot with poor air ventilation by pressing seven pallets in the backmost part of the container to one wall. The remaining space formed a gap of approximately 3 cm at the opposite wall. Three additional gaps of 2 cm, 3 cm and 4 cm between two pallets were created with spacers. Because pallet P11 was slightly deformed during the loading into the container by a forklift, an unwanted chimney with a size of 9 cm by 24 cm was created between pallets P9 and P11 (marked in orange). The additional gaps in our test setup are also marked in orange. The locations of the sensors are marked by small rectangles. The colors of the rectangles indicate the spatial distribution of the identified model parameters discussed in section 4. For clarity, only sensors in tier 5 (1.25m above the floor) are plotted. The 6 stacks of each pallet are marked by dotted lines. Some sensors were mounted at positions where the corners of 4 boxes meet in the middle of the pallet. Because they were mounted in the free space in the corners, and not between the bananas, their reaction to temperature changes resembles rather the reaction of other corners than of center positions.

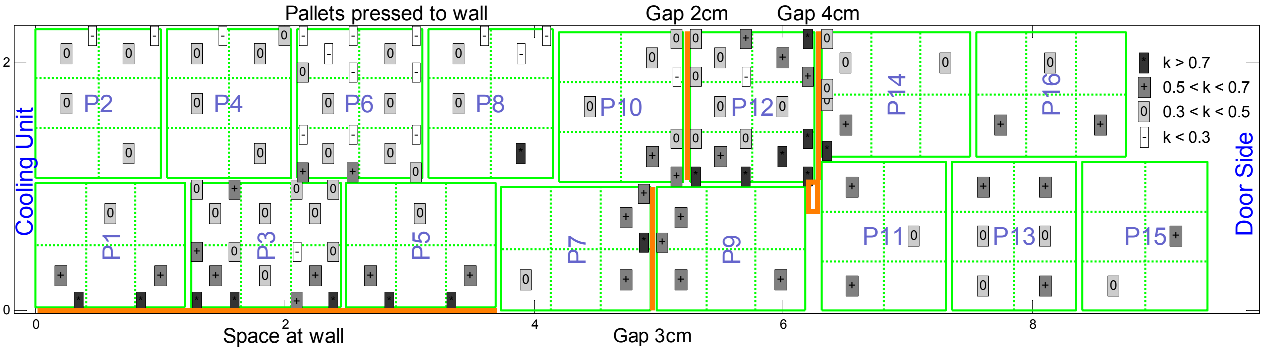


*Figure 3: Positions of the test pallets inside a 40-foot container. The 6 stacks per pallet are marked by dotted lines. The positions of the temperature sensors (tier 5 only) are marked by small rectangles. The background colors of the rectangles indicate the range of the identified model parameters (see section 3 and 4). Gaps between pallets are marked by thick orange lines.*

Further temperature records were available from earlier tests (Jedermann et al., 2011). These data sets contain the temperature history of sea transports from Central America to Europe in 2009 and 2011. Because only a limited number of data loggers were installed in the same center positions as in the current test, the data from the sea transports could only be used for model verification.

# 3. Mathematical model

A first evaluation of the tests over 5 days showed that a direct comparison of the temperature curves of different sensors is not possible. The temperature in the corners was affected by the initial temperature of the boxes, which varied between 13.8 °C and 14.6 °C. Furthermore, a satisfactory fit of the curves with a simple exponential time function was not feasible. For this reason, we fitted the curves with a mathematical model in order to characterize the cooling performance for each box by a numerical parameter.

The aim of the modeling is to describe the relations between the three types of measurement signals: the temperature of the supply air, the temperature in the corner of a box and the temperature in the center of a box. Two signals were considered as the model input and the remaining signal as model output. Most parts of the model could be described as a linear dynamic system, given by a set of differential equations. The only exception was the self-warming of the bananas, which depends on a non-linear function of the temperature (see section 3.2).

 http://dx.doi.org/10.1016/j.jfoodeng.2012.10.039

First order systems proved to be insufficient to achieve a good fit between the predicted and the measured output signal. With a second order system an acceptable fit was achieved. Higher order systems were avoided because, together with an increasing number of parameters, the system identification tends to become unstable, and it becomes more difficult to interpret the results.

There are several factors which make it almost unfeasible to establish an exact physical model of the temperature reaction of a stack of banana boxes inside a container, such as turbulent air flows, variations in the size of the gaps between the boxes, and the unknown thermal conductivity of a mix of bananas and air inside the boxes. Therefore, we focused on rather an empirical approach that is based only on some general physical considerations with the goal of predicting a close fit to the measured output signals. Because there is no unique or 'correct' model, different model structures were tested. Finally, we selected those which turned out to be the most useful for parameter identification.

The fast reaction of the corners to temperature changes and the slow reaction of the centers were described by two separate models. These two models can explain the observed differences in the speed of temperature change in the banana boxes in response to set point changes by the variation of only two parameters each. The underlying physical considerations of the model are as follows:

- The model consists of some time constants representing the thermal mass of the bananas, the box and the sensor itself. Because the thermal masses are the same for all banana boxes, the time constants should be independent from the positions in the container.
- A second set of parameters describes the part of the model which varies with the position of the box in the pallet and the packing of the bananas into the box. The air-holes might be blocked by other boxes or fully open. The width of the gaps between the boxes influences the ventilation as well. These parameters can be interpreted as coupling factors, describing how well the fresh air from outside is mixed with the air inside the box. These coupling factors vary for each box. They are the key parameters to interpret spatial temperature variations inside the container.
- In the long term, the output temperature approaches the input temperature. Therefore, the limiting value for the total system gain for infinite time should be about 1. This leads to the condition that the sum of a pair of mixing factors for one box has to be close to 1 as well.

## 3.1. Model for the temperature-time behavior of the corners

The model in Figure 4 predicts the temperature in one corner of a box as a function of time (corner temperature) $y_E(t)$. The model requires the temperature of the supply air $u_s(t)$ and of the center of the box $y_M(t)$ as inputs. The inputs are mixed with the coupling factor $k_1$. The resulting signal $u_1$ is the input to a serial connection of two first order delay elements with the time constants $T_1$ and $T_2$. The signals $x_1(t)$ and $x_2(t)$ are the outputs or states of the delay elements. The model output requires a second mixing element with the gain factors $c_1$ and $c_2$ with $c_1 + c_2 \approx 1$.

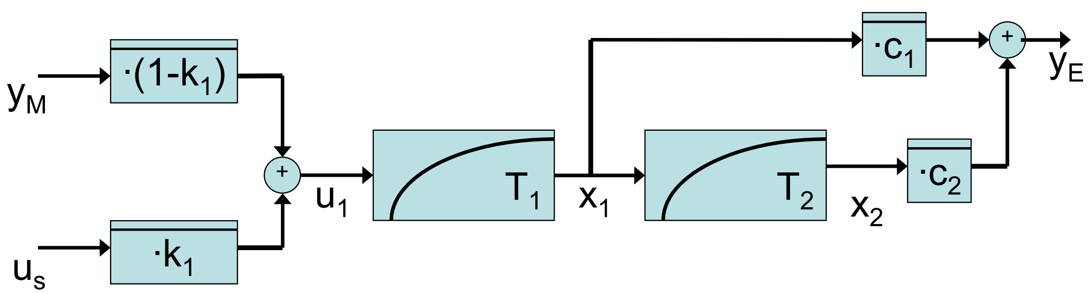


*Figure 4: Model structure to predict the temperature in one corner of the box ($y_M$=temperature of the center of the box, $u_s$=temperature of the supply air, $k_1$=coupling factor for the corner of a box, $u_1$=mixed input signal, $x_1$, $x_2$=outputs or states of the delay elements, $T_1$, $T_2$= time constants, $c_1$, $c_2$ =gain factors, $y_E$ =corner temperature)*

The model can be interpreted as a raw physical interpretation: the time constant $T_1$ describes the thermal mass of the air in the corner of the box and of the sensor itself; $T_2$ describes how fast the surface of the plastic film containing the bananas reacts to temperature changes. The sensor can be partly in contact with the film surrounding the bananas. Therefore, it measures a mixture ($c_1$, $c_2$) of the air temperature and influence of the banana surface temperature (Figure 5). The exact position of the sensor and an unwanted contact with the film is a random influence that could not be avoided in our experiments.


*Figure 5: Position of the sensor in the corner of a box. The measured temperature is influenced by supply air temperature, heat transfer through the cardboard box and warming of the supply air at the surface of the bananas.*

In order to simplify the system identification, $k_1$ was extracted to appear only once in the right term in equation (1):

$$u_1(t) = k_1 \cdot u_s(t) + [1 - k_1] \cdot y_M(t) = y_M(t) + k_1 \cdot [u_s(t) - y_M(t)] \tag{1}$$

The model structure in Figure 4 was translated to a state-space description (2):

$$\begin{aligned} \partial/\partial t \begin{bmatrix} x_1(t) \\ x_2(t) \end{bmatrix} &= A \cdot \begin{bmatrix} x_1(t) \\ x_2(t) \end{bmatrix} + B \cdot \begin{bmatrix} y_M(t) \\ u_s(t) - y_M(t) \end{bmatrix} \\ y_E(t) &= C \cdot \begin{bmatrix} x_1(t) \\ x_2(t) \end{bmatrix} \end{aligned} \tag{2}$$

with the parameter matrixes *A, B* and *C* (3):

$$A = \begin{bmatrix} -1/T_1 & 0 \\ 1/T_2 & -1/T_2 \end{bmatrix}$$
$$B = \begin{bmatrix} 1/T_1 & k_1/T_1 \\ 0 & 0 \end{bmatrix} \quad (3)$$
$$C = \begin{bmatrix} c_1 & c_2 \end{bmatrix}$$

In total, the model has 5 independent parameters. During an initial run of the identification process, the 5 parameters were estimated separately for all available corner measurements. A satisfactory curve fitting for different measured temperature curves is even possible, if the number of free parameters is reduced to 3. The 2 time constants were set to rounded average values of the first identification run with $T_1 = 0.3$ hours and $T_2 = 4$ hours. During a second identification run the remaining 3 parameters $k_1$, $c_1$ and $c_2$ were identified for each corner sensor anew.

## 3.2. Model for the center of the box

A similar model was used to predict the temperature in the center of the box (Figure 6). The model has the same input signals as the corner model, but a different coupling factor $k_M$ and different time constants $T_3$ and $T_4$. A second signal mixing at the output was not necessary.

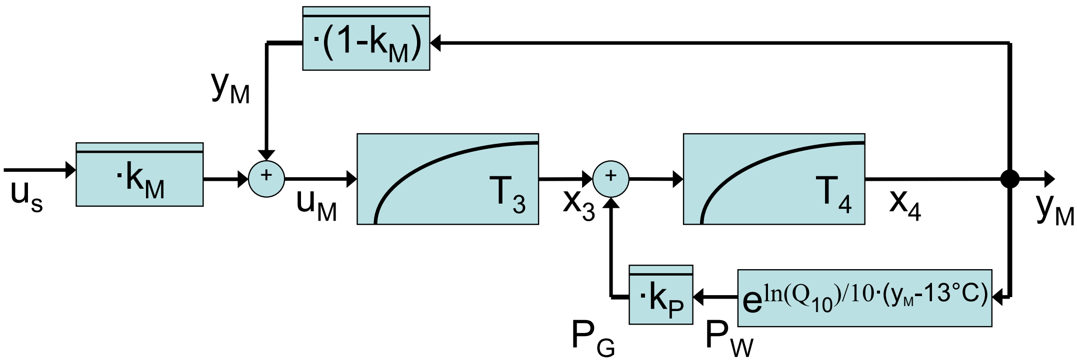


*Figure 6: Model structure to predict the temperature in the center of the box ($u_s$=temperature of the supply air, $k_M$=coupling factor, $x_3$, $x_4$=outputs or states of the delay elements, $T_3$,$T_4$= time constants, $k_P$=gain factor for the generated heat $P_G$=generated respiration heat, $P_W$=exponential respiration heat term, $Q_{10}$=change of heat production at a temperature change of 10 K, $y_M$=temperature of the center of the box)*

Because $y_M$ appears at the input as well as at the output of the model, the model entails an additional feedback loop. This model structure was selected because it simplifies the system identification.

A second non-linear feedback loop describes the self-warming by respiration of the bananas (Palafox et al., 2011). The generated heat increases with the temperature according to an exponential relation. The parameter $Q_{10}$ relates the change of heat production to a temperature change of 10 Kelvin (Fonseca et al., 2002). The generated heat at a certain temperature $P_G$ is calculated by equation (4). For simplification, the exponential term in equation (4) is named as $P_W(t)$:

$$P_G(t) = k_P \cdot e^{\frac{\ln(Q_{10})}{10} \cdot \left[y_M(t) - 13^\circ C\right]} = k_P \cdot P_W(t) \quad (4)$$

 http://dx.doi.org/10.1016/j.jfoodeng.2012.10.039

$Q_{10}$ was set to a value of 3, which gave a good fit for tests ashore as well as offshore. The selection of the $Q_{10}$ value is discussed in section 4.5. $P_W(t)$ can be calculated directly from the measured temperature in the center. The remaining unknown factor $k_P$ can be estimated by linear system identification techniques. If $P_W(t)$ is considered as an additional input to the system, the model can be translated to the following state-space description (5):

$$\partial/\partial t \begin{bmatrix} x_3(t) \\ x_4(t) \end{bmatrix} = A' \cdot \begin{bmatrix} x_3(t) \\ x_4(t) \end{bmatrix} + B' \cdot \begin{bmatrix} y_M(t) \\ u_s(t) - y_M(t) \\ P_W(t) \end{bmatrix}$$
$$y_M(t) = C' \cdot \begin{bmatrix} x_3(t) \\ x_4(t) \end{bmatrix} \tag{5}$$

with the parameter matrixes *A', B'* and *C'* (6):

$$A' = \begin{bmatrix} -1/T_3 & 0 \\ 1/T_4 & -1/T_4 \end{bmatrix}$$
$$B' = \begin{bmatrix} 1/T_3 & k_M/T_3 & 0 \\ 0 & 0 & k_P \end{bmatrix} \tag{6}$$
$$C' = \begin{bmatrix} 0 & 1 \end{bmatrix}$$

The center model contains 4 free parameters. The two time constants were set to constant values in a similar way as for the corner model. An initial fully free identification resulted in the following rounded average values of $T_3$ = 4 hours and $T_4$ = 15 hours. The higher values, compared to $T_1$ and $T_2$ of the corner model, show that the center reacts much more slowly to temperature changes. The remaining two parameters $k_M$ and $k_P$ were identified from the measured data for each box.

The parameter $k_P$ can be interpreted according to the following limit case: the model inputs $u_s$ and $y_M$ as well as the model states $x_3$ and $x_4$ are set to 13 °C. As long as the states remain close to 13 °C, most elements of the state-space description can be neglected, resulting in (7):

$$\frac{\partial y_M(t)}{\partial t} \approx k_P \cdot P_W(13°C) = k_P \tag{7}$$

Therefore, $k_P$ can be interpreted as the initial speed of temperature change (in °C/hour) generated by self-warming at 13°C.

## 3.3. System identification

The identification of the model parameters was carried out with the Matlab System Identification Toolbox (MathWorks, 2012). The 'pem' function applies an iterative **p**rediction-**e**rror **m**inimization at the output of the model. The elements of the parameter matrices can be set either to a fixed value or to a freely adjustable mode.

The prediction error is evaluated according to a fit-value calculated according to equation (8), with $y^*$ as model output, $y'$ as measured value, $\overline{y'}$ as average over time and *norm*() as the Euclidean length of a vector containing a time series:

$$fit = 100 \cdot \frac{1 - \mathrm{norm}\left(y^* - y'\right)}{\mathrm{norm}\left(y' - \overline{y'}\right)} \tag{8}$$

# 4. Application of the model to field test data

The model was applied to the temperature data recorded during the field test carried out in January 2012. As a first step, the $k_1$ parameters for the corner sensors of the boxes were identified, with the temperature of the center of the respective boxes as an additional input. The effectiveness of cooling mainly depends on the width of gaps between the pallets (see section 4.6 for a detailed discussion). Figure 7 shows 2 examples for the reaction of the corner sensors to changes of the set point, together with the temperature over time curves for the center of the box and the supply air. The reaction can have only small amplitude (Figure 7a) with a minimum $k_1$ value of 0.159 or fast reaction (Figure 7b) with a maximum $k_1$ value of 0.926. On average, a fit value of 91.5% was achieved for the corner model, with a standard deviation of ± 4.1%. If the fit values for different corner positions are compared, the lowest values were found at corners with low $k_1$ values because the resulting temperature changes, and thereby the signal-to-noise ratio, was also lower.

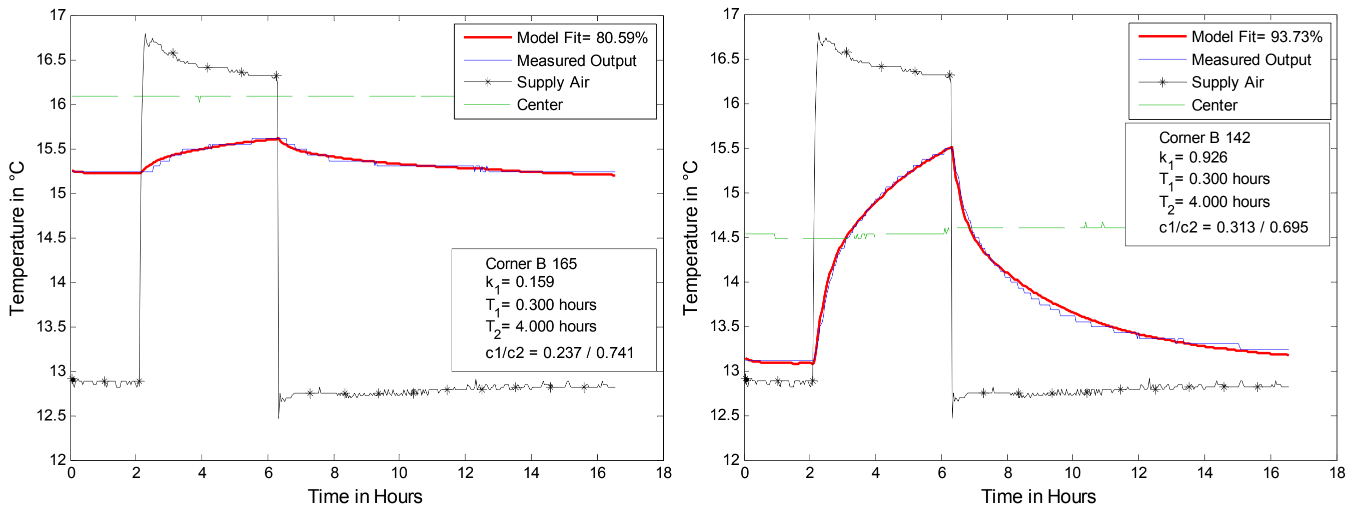


*Figure 7: Examples for the measured reaction of the temperature in the corners (blue) of two boxes towards a set point change (black). The model (red) achieves a good fit for reactions with low amplitude (a/LEFT) as well as with high amplitude (b/RIGHT). Curve (b) was measured close to a 3 cm width gap between pallets and wall; curve (a) at the opposite side of the container where the pallets were pressed to the wall.*

The boundary condition $c_1 + c_2 \approx 1$ was fulfilled with an average sum of 0.992 ± 0.012. The identified $c_1$ values were in a range between 0.17 and 0.73.

## 4.1. Identification of centers

The parameters $k_P$ and $k_M$ for the model of the temperature in the centers were estimated as the second step. The parameter $k_P$ for self-warming showed only little variation for different boxes, with an average value of 0.0434±0.0045. The values for $k_M$ varied between 0.286 and 0.751. Figure 8 shows two examples of a slow (Figure 8a) and a fast reaction (Figure 8b) of the center of the box to temperature changes. On average a fit value of 87.4% was achieved, with a standard deviation of ±3.3%.

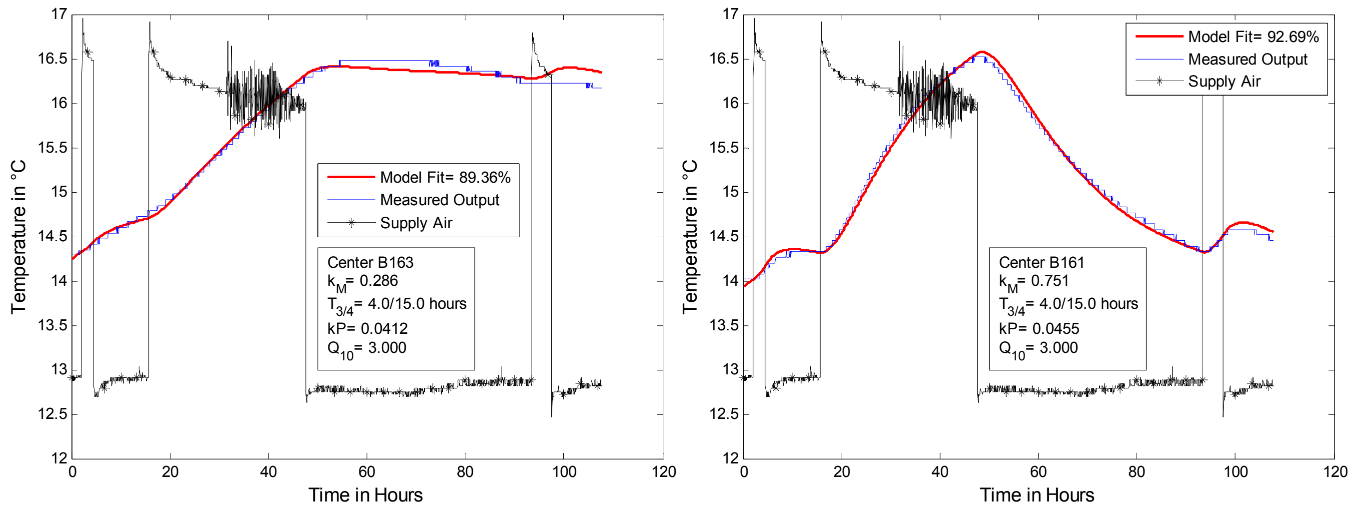


*Figure 8: Two examples for temperature curves for the center of the boxes. Model fit (red) for slow (a/LEFT) and fast (b/RIGHT) measured (blue) reaction of the box towards temperature changes of the supply air. Both curves were measured in pallet 8. Curve (a) at the wall-side and curve (b) at the opposite side.*

## 4.2. Relation between the coupling factors of the corners and the centers

According to the physical interpretation of our model, both parameters $k_I$ and $k_M$ depend on the amount of supply air that penetrates into the box. If this interpretation is true, there should be a relation between the average $k_I$ values of the 4 corners and the $k_M$ value for the center of the same box. The identified values of the 12 boxes, which had sensors in all 4 corners, are plotted in Figure 9:

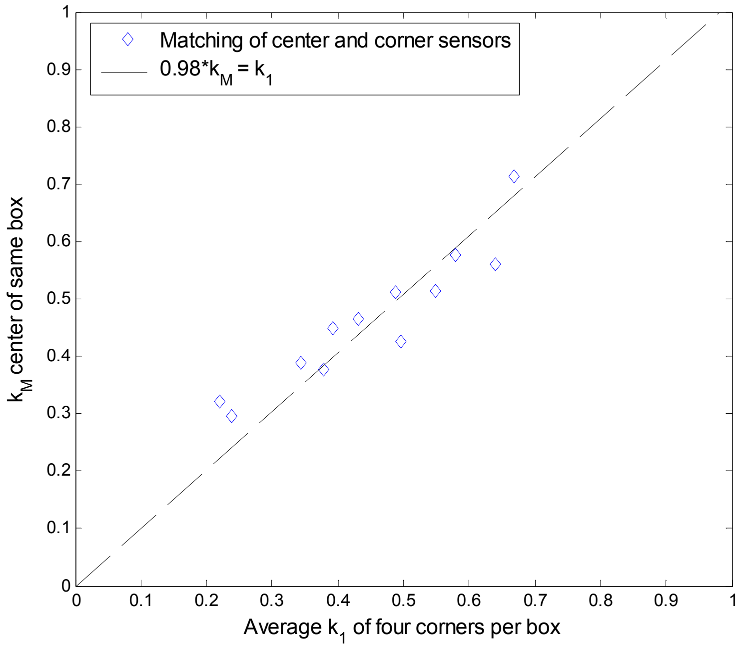


*Figure 9: Comparison of the identified coupling factors for the corners and the centers. The average of the $k_I$ values for the 4 corners of a box is nearly equal to the $k_M$ value for the center of the same box.*

Figure 9 shows an approximately linear relation with $R^2 = 0.85$ according to equation (9)

$$\overline{k_1} \approx 0.98 \cdot k_M \tag{9}$$

This linear relation can be applied in two ways: firstly, the $k_I$ and $k_M$ values can be directly compared; secondly, it is possible to measure the temperature only in the corners, where sensors are easier to install and show a much faster reaction. After identification of the $k_I$ values, $k_M$ can be calculated according to equation (9) and the temperature in the center can be predicted.

## 4.3. Application of the model to sea transports

After evaluation of the model based on the data recorded ashore, the model was applied to the data set from a real sea transport recorded in March 2011. The $k_P$ and $k_M$ values for different center positions were identified from the data with $Q_{10} = 3$. The resulting average value for $k_P = 0.0139 \pm 0.0024$ differs greatly from the previous test ashore with $k_P = 0.0434$. This point will be discussed in the next section. Figure 10 shows the measured temperature in the center of the boxes at different positions in the container. Three positions were selected, which represent the slowest, the fastest and a cooling speed close to the average $k_M$ of 0.524. The average is 14% higher than the average $k_M$ value measured ashore of 0.458, which indicates a better performance of the cooling system. This can be explained by the fact that there were no additional gaps installed during the tests on sea transports. Because there were only small variations in the $k_P$ value, all three curves in Figure 10 were plotted with the same average $k_P = 0.0139$. Our model for the center temperatures can be applied to a short test ashore as well as to real sea transports with duration of two weeks. Only the parameter $k_M$ needs to be varied in order to represent the temperature curves at different positions.

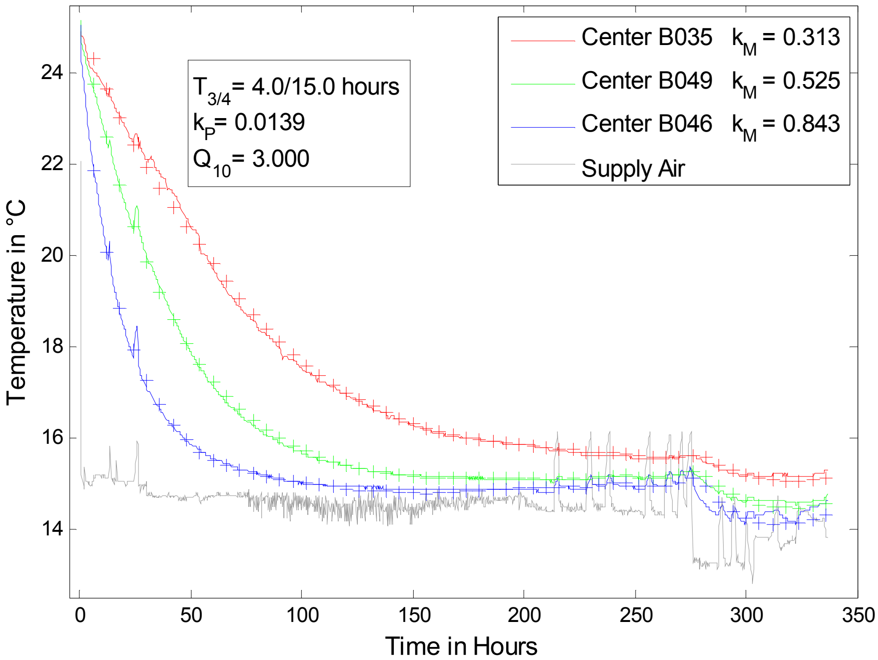


*Figure 10: Sea container test over 2 weeks. Examples of measured temperature curves (solid lines) and model fits (crosses) for the centers of three boxes. The measured temperature curves at different positions can be approximated by the same model; only the parameter $k_M$ needs to be adjusted.*

## 4.4. Analysis of factors influencing $k_P$

The biological activity of bananas and thereby the generated heat depends on the physiological state of the bananas, the temperature and the atmospheric conditions. Some containers are equipped with a special aggregate to provide a controlled atmosphere with reduced oxygen and increased carbon dioxide concentrations. In this case, the plastic film must have extra holes to enable gas exchange. Another way to reduce the biological activity is to apply a modified atmosphere, which is provided by plastic films with specific gas permeability. The film reduces the gas exchange. The oxygen concentration decreases and the carbon dioxide concentration increases by self-respiration. Table 1 lists the atmospheric conditions and the identified $k_P$ values of the previously described tests and one additional offshore test carried out in 2009.

 http://dx.doi.org/10.1016/j.jfoodeng.2012.10.039

| **Year** | **Test** | **Atmosphere** | $k_P$ |
|---|---|---|---|
| 2009 | Sea transport 2 weeks | Modified atmosphere ($CO_2$ 5% and $O_2$ 16%) | 0.0207 ± 0.0056 |
| 2011 | Sea transport 2 weeks | Controlled atmosphere ($CO_2$ 4.5% and $O_2$ 3%) | 0.0139 ± 0.0024 |
| 2012 | Ashore 5 days | No control, film with holes ($CO_2$ ~2%) | 0.0434 ± 0.0045 |

*Table 1: Atmospheric conditions and identified value $k_P$ for self-warming.*

The values in the table show that the best reduction of biological activity is achieved with a controlled atmosphere, whereas a plastic film with holes but without any atmosphere control is the worst case.

Because ambient temperature was lower than the temperature inside the container during the test ashore, isolation losses did not contribute as an additional heat source. The high value for $k_P$ can be explained by self-warming.

The value $k_P$, which gives the speed of temperature rise, can be re-calculated to the generated heat $W_G$ in Watts per ton according to equation (10), based on the specific thermal capacity of bananas of 3350 J/kg·K and 1 hour = 3600 seconds:

$$W_G(T) = 930.5 \cdot k_P \cdot e^{\frac{\ln(Q_{10})}{10} \cdot [T - 13^\circ C]} \qquad (10)$$

The values in Table 1 result in a heat production between 18 and 56 Watts per ton. Under the assumption of good cooling performance, the temperature of the bananas decreases with up to 0.075°C per hour at 16°C (Figure 8b), which is equivalent to a heat removal of 70 Watt per ton in addition to the removal of the heat generated by biological activity. In total, the cooling unit removes a maximum of 126 Watts per ton or 2.2 kW for a container loaded with 17.6 tons of bananas. This value is much lower than the available cooling capacity of 16.6 kW of the applied Thermoking Magnum Plus cooling unit. Therefore, it is evident that improvements in the cooling performance cannot be achieved by increasing the capacity of the cooling unit. Instead, it is necessary to improve the air flow between the pallets and into the boxes. Unwanted gaps and chimneys have to be avoided to provide a high air pressure difference between the supply and return air.

## 4.5. Setting of the $Q_{10}$ parameter

The $Q_{10}$ parameter cannot be estimated by linear system identification methods because it is part of a non-linear exponential function. A manual test of different $Q_{10}$ values showed that the model fit is improved by larger values for $Q_{10}$ with a maximum fit value of 88.8% for $Q_{10}$ =18. Typical values for $Q_{10}$ found in literature vary between 2.2 for green bananas (Kader 1987) and 3.5 for ripe bananas (Gross, 2004), in which heat production of ripening bananas is 3 to 4 times higher than that of green bananas (Kader 2012). As a compromise between biological requirements and optimization of the model accuracy we selected a value of $Q_{10}$=3, resulting in a fit value of 87.4%, which is only slightly worse than the maximum for $Q_{10}$ =18.

Setting an exact value for $Q_{10}$ is not crucial for our model because the model provides a good fit over a wide range of $Q_{10}$ values. The selected value of $Q_{10}$=3 gave a good fit for tests ashore as well as offshore. But this means, on the other hand, that our experimental setup and type of model is not suitable for an accurate estimation of $Q_{10}$. A reliable estimation of $Q_{10}$ would require detailed laboratory experiments with more than the two tested temperature levels of 13°C and 16°C, which is beyond the scope of our paper.

## *4.6. Influence of gaps on $k_1$*

In the following section we analyze the spatial dependency of the coupling factors $k_1$ for the corners and the influence of gaps on this parameter. The spatial analysis was only possible for the data recorded ashore because the earlier sea transportation tests focused on the box center temperatures with only 2 or 4 sensors mounted in corner positions.

The positions of the pallets, sensors and of the gaps for the test ashore are depicted in Figure 3. The rectangles for the sensor positions are filled according to a grey scale showing the spatial distribution of the identified coupling factors. Dark grey indicates good coupling to the air stream; white indicates poor ventilation. The $k_M$ values for the centers are marked in the same figure. The best cooling was achieved in the 4 cm width gap and in the gap at the wall. Table 2 shows the relation between the gap width and the average $k_1$ value of all neighboring sensors.

| Position | Measured at/between pallets | Average $k_1$ |
|---|---|---|
| Pallets pressed to wall | P2, P4, P6, P8 | 0.252 ± 0.065 |
| Gap at the wall 3cm | P1, P3, P5 | 0.782 ± 0.109 |
| Closed gap 0cm | P4/P6, P6/P8 | 0.315 ± 0.101 |
| Gap 2cm | P10/P12 | 0.485 ± 0.160 |
| Gap 4cm | P12/P14 | 0.630 ± 0.161 |

*Table 2: Average $k_1$ values for different gaps. For each gap 8 sensors in corner positions were available, over which the average of the identified model parameters was calculated.*

It can be clearly seen that there is a direct relation between the gap width and $k_1$. Minimum $k_1$ values were measured especially in the boxes near the gap with the pallets pressed to the wall. The small air flow leads to longer cooling times, higher transport temperatures and, therefore, higher physiological activity of these bananas. The air flow through a stack from bottom to top is limited because of the dense packaging and the plastic film around the bananas. In the worst case these bananas start ripening and the total container is lost because ripeness heat (up to 700 W/t) cannot be channeled away.

## *4.7. Application of the model*

Figure 8(a) indicates that the cooling unit fails to cool down the bananas to a temperature close to the set point, if the coupling factor $k_M$ is too low. The lowest temperature that can be achieved for a given set of index values after a long period of cooling can be calculated by simulating the model for the center. Alternatively, the model equations (5) and (6) can be transformed to directly calculate the relation between $k_M$, $k_P$, air supply temperature $u_{S\infty}$= 13°C and final center temperature $y_{M\infty}$. If the model arrives at a stable state after infinite time, the changes of the state variables $\partial x_{3,4}/\partial t$ should be zero. The center $y_M$ temperature is equal to the state $x_4$ because the output matrix of the system is $C'$=[0 1]. The temperature of this stable state depends only on the relation of $k_M/k_P$ in equation (11):

$$\frac{k_M}{k_P} = \frac{T_4 \cdot P_W(y_{M\infty})}{y_{M\infty} - u_{S\infty}} \qquad (11)$$

The pairs of index values $k_M$ and $k_P$ that were found during our 3 experiments offshore and ashore are marked by dots in Figure 11. Pairs of index values that lead to the same final temperature according to equation (11) are connected with blue lines. If the relation $k_M/k_P$ is lower than 4.481, the equation has no solution for $y_{M\infty}$ and a stable state condition does not exist. This is the case for low $k_M$ and high $k_P$ values in the hatched area. The heat generated by self-warming is greater than the amount of heat which can be removed by the cold air stream. Therefore, a hot spot is created; an increase of temperature cannot be prevented.

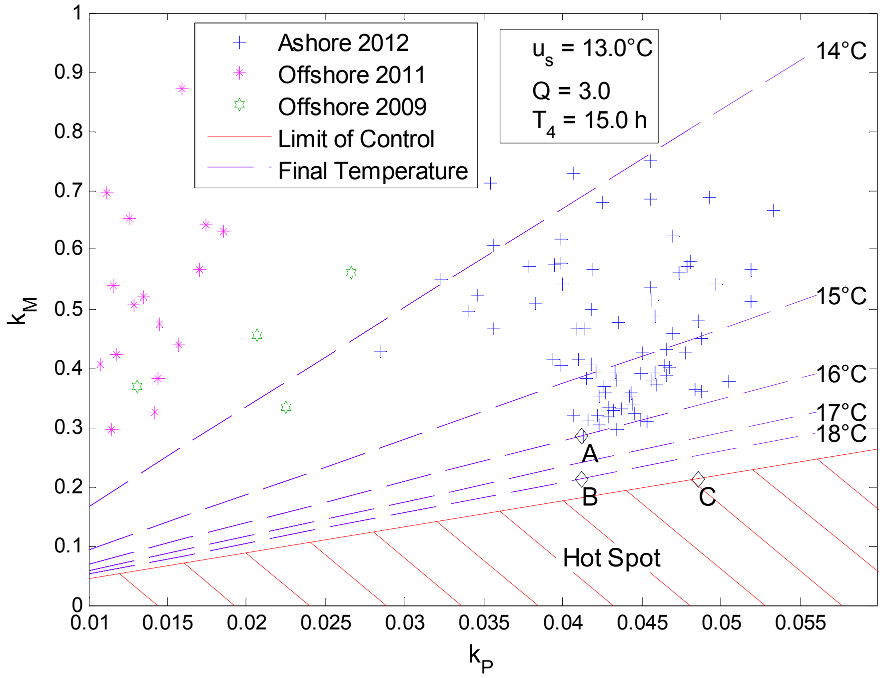


*Figure 11: Identified values of three experiments and calculated final center temperature after cooling according to equation (11). A stable limit case exists only for the $k_M/k_P$ combinations outside the hatched area; otherwise, a continued temperature increase cannot be prevented which results in a hot spot. A scenario for development of a hot spot by changes of $k_M$ and $k_P$ during the experiment is marked by the letters A, B and C.*

Point A marks one pair of index values that was identified from the temperature curves in Figure 8(a). The cooling unit cannot lower the temperature to a value less than 16 °C for this pair of index values, even if the duration is prolonged. Point A was taken as the starting point for the following example calculation:

If the coupling of this box ($k_M$) decreases by 25% by additional blocking of the air stream or loss of air pressure by unwanted chimneys, the minimum achievable temperature increases to 18 °C (Point B). If bananas remain at this temperature for a longer period of time, there is a high risk of starting an unwanted ripening process. If additional heat ($k_P$) is created by ripening, the process becomes uncontrollable (Point C).

## 4.8. Discussion

One main task of our project is to better control and to improve the cooling of food products during transport. As a prerequisite for better control, it is necessary to understand the patterns and factors influencing the spatial temperature distribution.

We developed two separate models to explain the temperature changes measured in either one corner or the center of banana boxes inside a pallet in a reefer container. Both models take the measured supply air temperature as first input. The corner model requires the temperature in the center as second input, whereas the center model requires the calculated thermal energy generated by biological processes as second input. The latter one can be calculated by either the measured or the predicted temperature of the center of the box.

Both models can be applied in two ways. Firstly, they can be utilized to identify a set of index values that characterize the performance of the cooling and the biological activity of the fruits, if measurement data for the supply air, center and corner temperature are available.

Secondly, the models can calculate a prediction for the center and corner temperature. For example, if the range of the $k_M$ parameter is known from a previous experiment (e.g. $k_M$ = 0.29 … 0.75), effects of changes in the set point, resulting in a different supply air temperature, or changes of the atmospheric conditions, resulting in different $k_P$ values according to Table 1, can be calculated by a simulation of the model equations. Conditions under which temperature-related quality defects appear can be detected by simulation of different sets of index values.

By application of the models to data recorded during field tests offshore and ashore, we can show that the models are suitable to explain the temperature over time changes of palletized bananas at different measurement positions.

Because the container was only loaded with 16 pallets for the tests ashore, the cooling performance and the $k_M$ values can be slightly lower for a fully loaded container with 20 pallets.

Furthermore, we can establish a relation between the coupling factors for the corner and the center model. By making use of the relation it is possible to identify the coupling factor for the corners, which requires only a few hours of measurement data, and thereby predict the long-term temperature development in the center.

The model for the generated heat by respiration $P_W$ as a function of temperature has to be further improved and validated. The inaccuracy can have different reasons: bananas are a living product with high biological variance; the green bananas in our test might have already started ripening and, thereby, the heat production increased disproportionately.

# 5. Summary

One of the key findings of our work is the introduction of a new method for evaluation of spatial temperature distribution. By this method, the measured temperature curves can be reduced to two index values, which give information about the performance of the cooling process.

- $k_I$ and $k_M$ indicate how well a banana box is coupled to the cold air stream provided by the cooling unit. Measured values were between 0.2 and 0.8, with higher values indicating a good cooling performance. The coupling factor for the corners mainly depends on the width of gaps between the pallets. Larger gaps result in better cooling of the adjacent side of the pallet, but they reduce the overall performance of the cooling by loss of air pressure.
- $k_P$ indicates how much heat is generated by biological activity of the bananas. The lowest values of 0.01 are achieved by a controlled atmosphere. In normal atmosphere, the values increase up to 0.05. Higher values can indicate the beginning of an unwanted ripening process. The comparison of the three experiments provides additional proof that controlled atmosphere conditions largely reduce the biological activity.
- A low value for the relation $k_M/k_P$ indicates that the box is close to a situation in which the generated heat cannot be channeled away and the risk of a hot spot increases.

The model provides a better understanding of spatial temperature conditions inside a reefer container loaded with fruits. It makes it possible to evaluate the effect of gaps between the pallets on the cooling performance. A homogenous distribution of gaps is crucial to maintain an even temperature and air flow throughout the container.

## 5.1. Acknowledgements

The research project “The Intelligent Container” is supported by the Federal Ministry of Education and Research, Germany, under reference number 01IA10001. Further information about the project can be found at http://www.intelligentcontainer.com. We additionally thank Ingersoll Rand Climate Control Technologies for provision of cooling equipment, and Dole Fresh Fruit Europe for provision of test facilities.

# 6. References


Billing, D.P., McDonald, B., & Hayes, A.J. (1998). Temperature characteristics within 20-foot reefer containers during export of New Zealand produce. *Refrigeration Science & Technology*, (2), 139-147.

Fonseca, S.C., Oliveira, F.A.R., & Brecht, J.K. (2002). Modelling respiration rate of fresh fruits and vegetables for modified atmosphere packages - a review. *Journal of Food Engineering*, 52, 99-119.

Gross, K.C. (2004). Summary of Respiration and Ethylene Production Rates. In K.C. Gross, C.Y. Wang, & M. Saltveit (Eds.), *The commercial storage of fruits, vegetables, and florist and nursery stocks.* Agriculture Handbook (66), U.S. Dept. of Agriculture, USA.

Ingersoll Rand Climate Control Technologies (2008). *TK 60275-4-MM Magnum+ Maintenance Manual*.

Jedermann, R., Becker, M., Görg, C., & Lang, W. (2011). Testing network protocols and signal attenuation in packed food transports. *International Journal of Sensor Networks (IJSNet),* 9, 170-181.

Jedermann, R., Moehrke, A., & Lang, W. (2010). Supervision of banana transport by the intelligent container. In *Coolchain-Management, 4th International Workshop* (J. Kreyenschmidt, Ed.), pp. 75-84, University of Bonn, Germany.

Kader, A.A. (1987). Respiration and Gas Exchange of Vegetables. In J.Weichmann, (ed.) *Postharvest Physiology of Vegetables*, Marcel Dekker, New York.

Kader, A.A. (2012) Banana - Recommendations for Maintaining Postharvest Quality. Department of Plant Sciences, University of California. Webpage available at http://postharvest.ucdavis.edu/PFfruits/Banana/.

MathWorks (2012). *Matlab R2012a Documentation - System Identification Toolbox - Identifying State-Space Models.* The MathWorks, Inc., Massachusetts, USA.

Moureh, J., & Flick, D. (2004). Airflow pattern and temperature distribution in a typical refrigerated truck configuration loaded with pallets. *International Journal of Refrigeration*, 27, 464-474.

Palafox-Albarrán, J., Jedermann, R., & Lang, W. (2011). Energy-Efficient Parameter Adaptation and Prediction Algorithms for the Estimation of Temperature Development inside a Food Container. In A.J. Cetto, J.-L. Ferrier, J. Filipe (Eds.), *Lecture Notes in Electrical Engineering - Informatics in Control, Automation and Robotics* (pp. 77-90). Springer, Berlin.

Rodríguez-Bermejo, J., Barreiro, P., Robla, J.I., & Ruiz-García, L. (2007). Thermal study of a transport container. *Journal of Food Engineering*, 80, 517-527.

Tanner, D.J., & Amos, N.D. (2003). Heat and Mass Transfer - Temperature Variability during Shipment of Fresh Produce. *Acta Horticulturae*, 599, 193-204.